New Approach for Integrity Bounds Computation Applied to Advanced Precise Positioning Applications

Navarro Madrid, P. F., Laínez Samper, M. D., Romay Merino, M. M., *GMV*

BIOGRAPHIES

Pedro F. Navarro Madrid has a Master of Science in Mathematics from the University of Murcia (Spain) and Postgraduate studies in Theoretical Physics at the University of Valencia (Spain). He has worked at GMV since 2002 as an engineer in the development of Galileo and later in R&D activities covering both the ground and user segments.

María D. Laínez Samper is currently coordinating the GMV research activities in the field of Satellite Navigation, and in particular those related to precise positioning applications. She has also worked in experimentation and verification activities, in the Operational Systems Division, during the preliminary phases of the Galileo Program, and has been the responsible for the clock prediction and navigation message computation modules in the Galileo E-OSPF (Experimental Orbitography and Synchronization Processing Facility).

Miguel M. Romay Merino is the GNSS Business Unit Director at GMV Aerospace and Defence. Miguel leads the GMV Unit that has become one of the strongest groups of GNSS experts thanks to its key involvement in GPS, EGNOS and Galileo. Miguel has been a pioneer in the Galileo Program, collaborating on aspects such as constellation design, precise orbit determination, integrity, performance evaluation, system definition, etc. Miguel is today involved in GMV research activities in the definition of novel GNSS applications and on the design of new generation GNSS.

ABSTRACT

Precise Point Positioning (PPP) is a consolidated high precision positioning technique providing centimetre-level error. PPP processes dual-frequency pseudorange and carrier-phase measurements from a single user receiver, using detailed physical models and precise GNSS orbit & clock products calculated beforehand. PPP is different from other precise-positioning approaches like RTK in the sense that no reference stations are needed for obtaining the positioning solution. Another advantage of PPP is that since the GNSS orbit & clock products are global, the PPP solutions are global as well. PPP can be applied at post-processing level and also in real-time applications, provided that real-time input orbit and clock data are available. Our GNSS team has developed the algorithms and the data processing infrastructure needed for providing a real-time PPP service. All the required components, from the real time orbit and clock products generation, to the PPP filter implementation and the service management, are under our responsibility.

In some previous works, we laid down the foundations for an upper-level reliability concept for PPP, closely linked to the final user perspective, with the aim of providing a certain reliability bound for the required applications. The initial integrity/reliability concept for PPP has now been mathematically rigorously reformulated and is introduced in this paper. The current formulation incorporates all the initially identified relevant indicators, and is expressed as a generalization of the patented IBPL (Isotropy-Based Protection Level) technique to sequential estimation processes.

In order to illustrate the excellent bounding capabilities of the new approach for PPP integrity/reliability computation, three different scenarios have been considered: static, kinematic and convergence. Results about the performances of the provided bounds are going to be provided in each one of the considered cases, in terms of protection level magnitude, percentage of integrity failures and safety index versus number of integrity failures.

INTRODUCTION

As in any positioning navigation system, integrity monitoring, together with accuracy and availability, is important for the PPP technique, and essential for the provision of certain critical applications. Different integrity concepts have been defined for the different satellite navigation solutions. GNSS integrity can be provided both at system and at user level. System integrity is based on the capability of the GNSS to collect and check indicators, in order to warn the user in case some anomaly is detected. The system should be able to alert the user any time the error of the estimated position exceeds a pre-determined limit, usually called alert limit. Otherwise, we would say that an integrity failure has

occurred, with the associated the potential risk of hazardously misleading information transmission to the user. But in many cases, it is not an anomaly in the system what might cause an inaccurate positioning solution, but a local effect in the user environment. In order to cope with these situations, integrity concepts at user level have also been formulated. It is the case of RAIM (receiver autonomous integrity monitoring), which is based on the consistency of the different computed positions with different subsets of redundant satellite measurements, as far as they are available. Besides this, and tightly related to the final application, additional sources of information for complementing the integrity data can be considered, like consistency checks with non-GNSS measurements, for example.

In our previous work we have laid down a general integrity concept for the PPP solutions, following a practical service oriented approximation. With this we mean that it should be focused neither on the system integrity nor on the integrity at user level only, but on the most favourable combination of significant indicators we can assess. The feasibility of such an integrity algorithm has been shown with a preliminary version, which was empirically tuned after identifying the best indicators of the quality of the PPP solution. See [Ref. 9.],[Ref. 10.] and [Ref. 11.].

This paper presents a new approach to monitor the integrity of PPP solutions that builds upon the concept described above. As a major step forward with respect to the preliminary version of the algorithm, the new revised formulation has now a sound statistical foundation and can compute real-time horizontal and vertical bounds to the positioning errors up to any user-defined level of confidence. The autonomous version uses indicators obtained at user level, as the measurement residuals statistics. But it is also designed to incorporate external data obtained from the system side. In this way, the computation can combine all the pieces of information relevant to achieve the best compliance with the given positioning service integrity requirements. The new method has grown as an evolution of the IBPL technique (Isotropy-Based Protection Level, see [Ref. 14.]), which assumes basically no a priori knowledge on either the size or the pointing direction of the vector of measurement errors, and offers a practical rule to compute error bounds from the measurement residuals. IBPL has proven highly reliable in all kinds of environments thanks to the simplicity of its assumptions, but its use is restricted to least-squares navigation. Then, the core idea of IBPL has been extended in order to provide meaningful bounds for a Kalman-filtered solution as PPP, taking into account important effects as the temporal correlation of measurements.

The technique described in this paper has been also adapted and applied to Kalman navigation with a low-cost receiver, where an extended validation campaign has shown excellent performances, even in urban environments (see [Ref. 16.]). For PPP, the method has been tailored after a careful analysis of the factors that degrade the accuracy of a PPP solution, such as the quality of the real-time orbit and clock products.

In addition to discussing the key concepts and ideas behind the proposed algorithm, we present the results of a dedicated experimentation campaign. We use *magicPPP*, our in-house PPP solution, to perform accuracy versus integrity analyses.

As our solution relies on an appropriate statistical estimation of the navigation errors, it can provide tight error bounds for a wide range of confidence levels. At the same time, it covers the degradation of the PPP solution in difficult environments, as the results of the experimentation will show.

In summary, after assessing the feasibility of an integrity concept for PPP we have developed a mathematically rigorous formulation that considers the different sources of error affecting the PPP solution. This formulation gives a method to compute bounds according to the available indicators, which performs very well from the point of view of integrity and availability. The approach introduced in this paper offers an opportunity for the provision of high-precision services with integrity for a wide range of applications, in the fields of agriculture, transport, construction, etc.

THE PPP TECHNIQUE AND *magicPPP*

PPP is a position location process which performs precise position determination using undifferenced, dual-frequency observations coming from a single GNSS receiver, together with detailed physical models and corrections, and precise GNSS orbit and clock products calculated beforehand. The quality of the reference orbits and clocks used in PPP is critical, as it is one of the main error sources of the positioning solution. Apart from observations and precise reference products, PPP algorithm also needs several additional corrections which mitigate systematic effects which lead to centimetre variations in the undifferenced code and phase observations, for example phase wind-up corrections, satellite antenna offsets, station displacements due to tides (earth and oceanic), etc.

The observations coming from all the satellites are processed together in a process that solves for the different unknowns; the receiver coordinates, phase ambiguity terms, the receiver clock offset and the zenith tropospheric delay. Most implementations of PPP algorithms use a sequential filter in which the process noise for the coordinates is adjusted depending on the receiver dynamics, the time evolution of the clock is more or less unconstrained (white noise with a high sigma), and the process noise for the tropospheric delay is adjusted to standard tropospheric activity. In the case of phase ambiguities, they are considered as a constant per pass.

Other implementations feature a batch algorithm instead, and therefore no process noise has to be modelled. In this case, the receiver clock offset is estimated at every measurement epoch, the coordinates are adjusted for the entire observation interval (static mode) or per epoch (kinematic mode), the troposphere is estimated at regular fixed intervals and the ambiguities are estimated per pass.

PPP is not a differential technique, it provides absolute positioning. On the one hand, integer carrier phase ambiguities cannot be obtained immediately after the PPP process has started (as it can be done for precise relative positioning techniques, i.e. RTK). PPP requires longer observation times for ensuring convergence has been achieved. On the other hand the PPP provided positioning solution is absolute, which can be a great advantage for many applications. The accuracy of RTK technique for absolute positioning applications has to be estimated combining the RTK positioning technique accuracy and the accuracy of the known position of the base station.

PPP has been normally conceived as a global service, taking into account that the orbit and clock products are themselves global. However, regional PPP services can also be provided, by feeding the PPP process with orbit and clock products generated from a non-global tracking network.

GMV has developed a proprietary PPP solution, which is called *magicPPP*, and provides an off-line PPP service as well as a RT PPP service. The PPP reference products generation is a complex process, especially for the demanding real time *magicPPP* service. The off-line *magicPPP* service is fed with products automatically generated processing data from a network of around 50 stations worldwide. The real time products generation process retrieves, from a worldwide station network, via Networked Transport of RTCM via Internet Protocol (www.rtcm-ntrip.org), NTRIP, dual-frequency code and phase measurements in real time. A high-level layout of the real time reference products generation infrastructure developed by GMV is shown in the figure below:

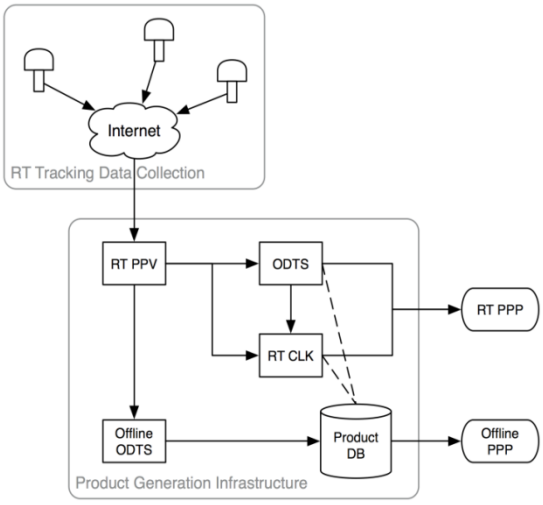

Figure 1: RT Product generation infrastructure

The reference product generation is based on an Orbit Determination and Time Synchronisation (ODTS) process. The GMV proprietary tool in charge of this process is *magicODTS*, which is part of the *magicGNSS* suite. *magicGNSS* is an OD&TS web tool (see http://magicgnss.gmv.com), able to compute multi-GNSS products.

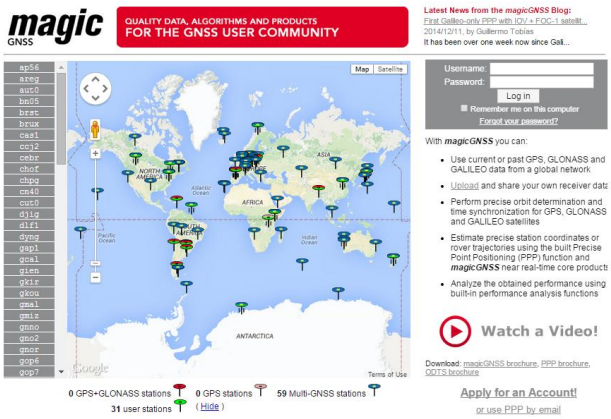

Figure 2: *magicGNSS* OD&TS tool

See [Ref. 3.] and [Ref. 4.] for further information about *magicGNSS*.

Back in 2010, GMV started participating as Analysis Centre for the Real Time IGS Pilot Project (http://www.rtigs.net/index.php), by processing data from a worldwide network of stations and providing precise predictions of GPS and GLONASS orbits and clocks, which are calculated using magicGNSS. Its contribution is still ongoing once Real Time IGS Project became operational in 2012. Both GPS and GLONASS are processed simultaneously. GLONASS inter-channel biases are estimated in order to compensate for the different internal delays in the pseudorange measurements through the GLONASS receiver, associated to the different frequencies used by the different satellites. Standard 2-day-long ODTS processes are executed every 15 minutes in order to generate real time orbit predictions, whereas real time clock data are generated at 1 second execution rate, via an auxiliary RT_CLK process, which estimates the satellite clocks in real time taking as input the pre-processed observations coming and the outputs from the last ODTS execution. The real-time orbits and clocks generated this way can be used for feeding *magicGNSS* RT PPP processes, and can be stored in standard formats (SP3, clock RINEX) for post-processing analyses.

As shown in Figure 1, the *magicGNSS* products generation includes the execution of an offline ODTS process which runs in off-line post-processing mode with a latency of 2 days and specific setup. It generates orbit and clock products more accurate than the real time ones. When available, they can be used for feeding off-line PPP processes.

The comparison of the off-line products, orbits and clocks, with IGS is shown in Figure 3. Typical orbit accuracy is about 6 cm, RMS, and clock accuracy is about 0.25 ns, RMS. For GLONASS, the analogue comparison has been carried out by comparing the off-line *magicGNSS* products with respect to ESOC (European Space Operations Centre) products. The orbit RMS stays around 10 cm, and the clock RMS stays around 0.4 ns, as shown in Figure 4.

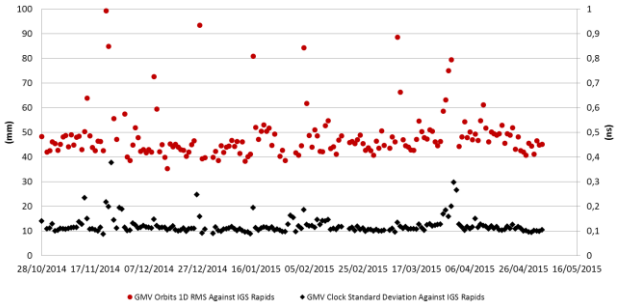

Figure 3: GPS Orbit and Clock comparison between IGS products and off-line magicGNSS products for October 2014-May 2015

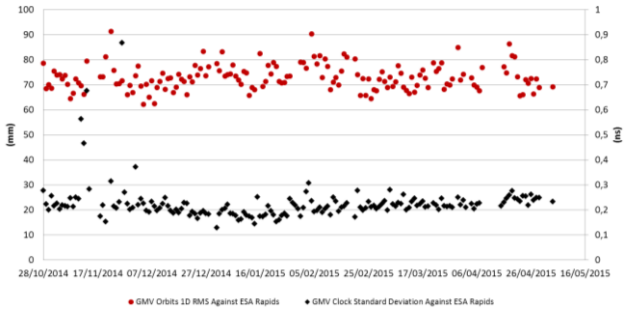

Figure 4: GLONASS Orbit and Clock comparison between ESOC products and off-line magicGNSS products for October 2014-May 2015

magicGNSS does also process Galileo data. Precise orbit and clock products can be computed, and fed into PPP processes. The first PPP results obtained with *magicPPP* with Galileo are reported in [Ref. 10.]. See [Ref. 7.] and [Ref. 10.] for further information about the *magicPPP* off-line and real time services.

PPP PROCESSING MODES

The PPP algorithm has traditionally used the iono-free combination of measurements at two different frequencies to cancel the ionospheric delay. This is a reasonable approach, since the ionospheric delay is not easy to model and estimate, in contrast with the case of the tropospheric delay. However, the iono-free combination has almost three times the noise of a single-frequency measurement. Thus, the option of using measurements of different frequencies in the PPP, while correcting and/or estimating the ionospheric delay, should be also considered. In fact, the results presented in the following sections show that this second processing mode improves the convergence of the PPP algorithm after the carrier-phase tracking is reset for several satellites (e.g. when passing under a bridge). Furthermore, this convergence can be improved by using the fact that the jump in the ambiguity after the gap must equal an integer number times the wavelength of the signal ("gap bridging").

Our tool *magicPPP* has an implementation of each of these two processing modes:

- Iono-free.
- Dual-frequency (with gap bridging).

The integrity algorithm provides Protection Levels in all cases. The results presented in the current work have been obtained by processing different scenarios in both processing modes.

PRELIMINARY STEPS FOR PPP INTEGRITY

The observed robustness of the PPP processes and the high accuracy of the obtained solutions motivated us to investigate on integrity algorithms for PPP. We have been working since 2012 in order to lay down a general integrity concept for the PPP solutions, following a practical service oriented approximation. With this we mean that we were not restricted to either pure system integrity or to integrity at user level only. Instead, we were looking for the most favourable combination of significant indicators we could assess. We started performing accuracy versus integrity analyses, trying to detect and study the different failure modes of the PPP processes. We analysed the PPP processes in detail, understanding that essential limitations for the attainable performances were linked to geometrical effects of the GNSS constellation, the quality of the orbit and clock products used as inputs, and the real-time reference systems realization. Relevant indicators were identified, and a preliminary integrity/reliability algorithm was designed.

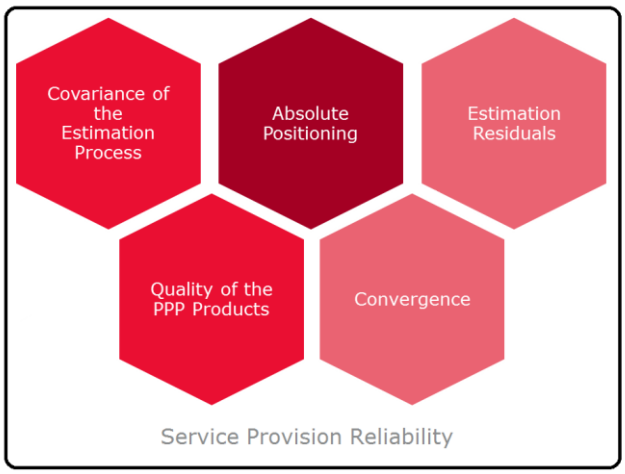

Figure 5: Preliminarily identified PPP integrity/reliability indicators

Then the system was empirically tuned and evaluated in several field scenarios emulating real time operations, including static and kinematic use cases, different visibility conditions (open sky and occultation with

different types of obstacles such as trees or buildings), and communication losses of different durations. Figure 6 below shows the preliminary PPP integrity/reliability algorithm performances, vertical protection level (PL) versus vertical error, in a kinematic scenario:

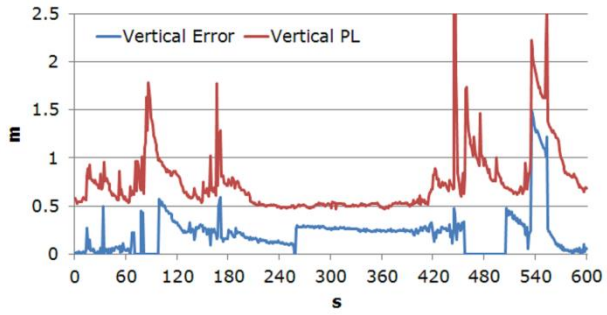

Figure 6: Preliminary PPP integrity/reliability algorithm performances: vertical PL vs error

We got to conclude that it should be feasible to define a specific algorithm able to bound the PPP errors, taking into account the identified relevant indicators, providing vertical and horizontal protection levels in the range of a few decimetres, with a low percentage of integrity failures. The weakness of the preliminary algorithm, though it worked quite well, was that it lacked a rigorous mathematical formulation. It followed an 'ad hoc' expression which had been empirically tuned for fitting all the analysed scenarios. The challenge was there: finding a comprehensive approach, statistically sound and mathematically rigorous, able to replace the observational preliminary computation, allowing testing the PPP integrity concept with high confidence levels and paving the way for a possible certification for safety of life users. Further details can be consulted in the following references: [Ref. 9.],[Ref. 10.] and [Ref. 11.].

GENERAL INTEGRITY METHOD FOR A KALMAN FILTER NAVIGATION SOLUTION

The task of building an integrity algorithm as described above, based on solid foundations, requires solving two main problems:

- Statistically characterize the different error sources: measurements, PPP products, etc. If possible, in real-time: for instance, measurement errors should be characterized by using the PPP residuals indicators.
- Compute a statistical distribution of the solution error that combines the different error sources according to the Kalman equations.

In fact, the general solution to these problems applies for any Kalman navigation solution. The particularities of the PPP algorithm will be later taken into account to tailor this general method.

The starting point to define such a method has been the IBPL technique (Isotropy-Based Protection Level), an integrity method for PVT least-squares solutions that has successfully addressed the associated difficulties (see references [Ref. 12.], [Ref. 13.], [Ref. 14.], [Ref. 15.] and associated patent [Ref. 1.]). The IBPL method assumes basically no a priori knowledge on either the size or the pointing direction of the vector of measurement errors, which leads to the so-called isotropy assumption that all possible pointing directions are equally probable. IBPL has proven highly reliable in all kinds of environments thanks to the simplicity of its assumptions. Although IBPL only applies to a least-squares solution, its ground idea and its mathematical development are very useful in the general approach to the filtered case, as well as providing a sound statistical characterization of the measurement errors.

In the case of a solution obtained from a Kalman-filter the new technique must address several additional challenges:

- The integrity bounds should reflect the improved filter performance, being much smaller than those computed for the least-squares.
- The filter makes use of different types of measurements: pseudoranges, carrier-phase, with different characteristics of noise.
- The filter solution combines observations from different epochs, in a possibly changing environment.
- The temporal correlation of measurements, which has a great impact in the performance of the filtered solution, must be accounted for.

The solution to these problems begins by defining a good set of probability distributions to characterize the individual error contributions (e.g. error introduced at one epoch by measurements of one type) and the global solution error. Multivariate t-distributions appear naturally in the context of the IBPL algorithm, as have been shown in the previous section. In addition, they provide an estimation of the errors covariance but also an indicator of the confidence that this assessment deserves. In fact, they are the simplest distributions with such properties. The new integrity algorithm for Kalman solutions, which will be called *Kalman Integrated Protection Level* (KIPL), is based on the use at different levels of t-distributions.

Next, it is important to understand how the Kalman filter combines observations of different types at successive epochs. The total error of the Kalman filter estimation is a sum of contributions due to several sources of error: pseudorange noise, carrier-phase noise, satellite navigation products, etc:

$$E = \sum_i E_{S_i}$$

The most important terms are the measurement errors. For each error measurement type S, the evolution of its contribution to the total error, E_S, may be analysed separately. At each new epoch k, the vector E_S is updated according to the following expression derived from the Kalman formulae

$$E_S = K e_S + (I - KH) \cdot F \cdot E'_S$$

where E'_S holds the previous value, K is the Kalman gain, F the state transition matrix, H the observation matrix, and e_S the measurements error vector at epoch k.

The first building block of KIPL is the computation of the t-distribution that characterizes the single epoch term Ke_S. In the case of the measurement errors, the parameters n and Σ that define the distribution are obtained from the measurement residuals computed at the current epoch, as follows:

$$n = n_{OBS} - d_{eff}$$
$$\Sigma = r^2 \cdot KW^{-1}K^T$$
$$r^2 = y^T W y / N$$

Here n_{OBS} is the number of measurements of type S, y the vector of residuals, W the measurements weight matrix and P the updated filter covariance matrix. The parameter d_{eff} is the *effective* number of estimated parameters; in the least-squares it coincides with the number of estimated parameters, in the Kalman filter it is smaller and is computed from the internal filter matrices. In the case of other sources, the values of n and Σ may be obtained in a different way.

The other essential ingredient is a method to update the t-distribution associated to E_S. It combines the two t-distributions for current epoch errors (Ke_S) and accumulated errors ($(I - KH) \cdot F \cdot E'_S$). In simple terms, it is based on a method to 'sum' two t-distribution defined by parameters (N_1, R_1) and (N_2, R_2) into a new one given by (N, R). KIPL provides a way to compute such sums in a sound and stable way. It takes into account the temporal correlation of measurements, which is a fundamental requirement to calculate appropriate bounds to the Kalman solution errors.

Finally, once the t-distribution for the solution errors is known, it is straightforward to obtain the protection level associated to a given confidence level. As the method is based on modelling the distribution of errors, rather than putting fairly conservative limits, it provides tight integrity bounds and is suited both for high and low confidence levels.

The method presented here, named KIPL (Kalman Integrated Protection Level), has been applied to the case of a GNSS low cost multi-constellation receiver, with excellent results (see [Ref. 16.]). GMV has filed a patent application at the European Patent Office, which is currently pending ([Ref. 2.]). In the next sections, we focus on the use of this method for the PPP algorithm.

PPP BOUNDING COMPUTATION

The computation of the bounds (Protection Levels) to the PPP solution is an application of the new method developed for any sequential estimation of position. In addition, it incorporates all the experience gathered in the previous phase on the indicators that provide relevant information about the quality of the solution. Figure 7 reflects the process that has led to the final form of the algorithm.

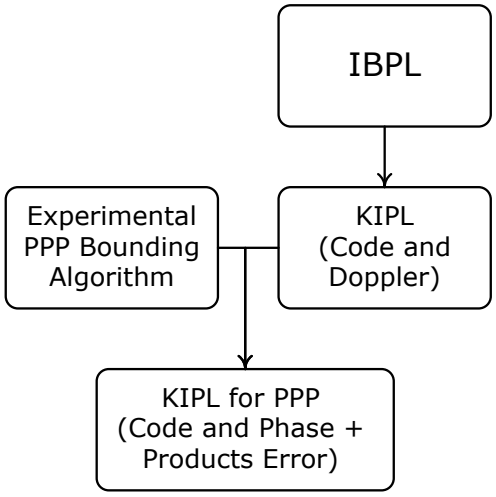

Figure 7: Schema of PPP integrity method development

The general algorithm is tailored to the PPP solution by incorporating the relevant parameters previously identified:

- Residuals statistics, being essential to characterize the measurement errors at each moment.
- Products quality. This information is expected to be supplied at the system side. It should take into account factors as the age of the real-time corrections.
- Measurements temporal correlation.
- Expected absolute error. This term refers to the error in the real-time reference frame realizations, although it can also absorb other unmodelled effects.

The basic parameters of some of these contributions can be refreshed in real-time based on suitable indicators, or take a priori values derived from previous characterizations.

Other indicators such as the covariance matrix and the convergence time appear implicitly as a result of the rigorous mathematical formulation of the algorithm.

ABSOLUTE vs RELATIVE POSITIONING, OFF-LINE vs REAL TIME POSITIONING

Just before entering into the details of the test cases carried out for proving the performances of the formulated integrity/reliability algorithm, let's stop one second and give a thought to the difference between absolute and relative positioning concepts, as well as to the difference between off-line back-office solutions and real time navigation.

In relative positioning, position solutions are provided with respect to the local base station or stations. Relative positioning techniques are: RTK, WARTK (Wide Area RTK) and classical DGPS (DGNSS). In absolute positioning, position solutions are provided with respect to a certain reference frame. Absolute positioning techniques are: GNSS stand-alone, for standard accuracy and PPP for high accuracy.

This means that if a relative positioning solution and an absolute positioning solution were to be compared, in terms of accuracy, a measurement of the uncertainty in the realization of the reference frame should be considered. This uncertainty is directly included in the error of the absolute positioning, whereas it is not included in the relative positioning error, since it cancels out in the differenced solution, but it reappears whenever the obtained relative position is required to be translated into an absolute measurement, which can happen for some applications, and not for others.

In order to illustrate the magnitude of the uncertainty in the reference frame realization we are discussing, we have performed a very simple non-exhaustive analysis consisting of measuring the accuracy of the ERPs (Earth Rotation Parameters) as re-estimated in the OD&TS process associated to the PPP orbit and clock products generation. Initial daily ERP values are input to the OD&TS process, as published by IERS, see [Ref. 20.], including estimations for the past days and predictions for the future. The re-estimation of the ERPs, see [Ref. 21.], implies a four-point interpolation for intermediate epochs ERPs computation. We have compared the re-estimated values of predicted ERP values (one and two day predictions) implied in the interpolations, with respect to subsequently published final estimations, and we have obtained the following results for the Xp and Yp pole coordinates:

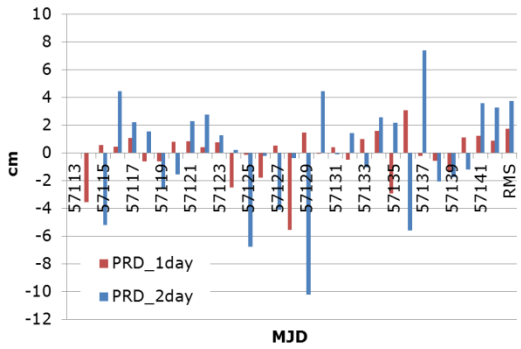

Figure 8: Xp prediction accuracy

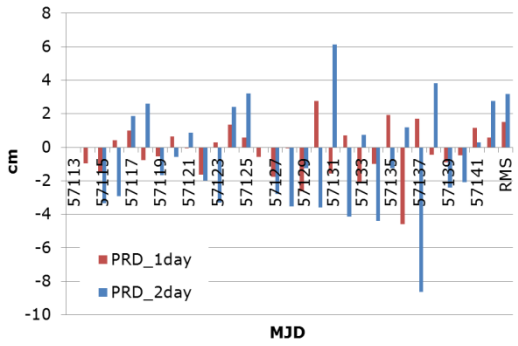

Figure 9: Yp prediction accuracy (0 deg latitude).

It can be observed that, though in terms of RMS the errors in the Xp and Yp parameters predictions are small, below 2 cm for 1-day-long predictions, and below 4 cm for 2-day-long predictions, isolated values can reach larger levels, up to 10 cm, and even larger for the universal time parameter UT1-UTC, which is not included for space reasons. This means that it is completely acceptable to state that real-time reference frame realizations can have typical errors of few centimetres, which is directly translated into the attainable accuracy of a real-time PPP process.

Furthermore, real-time PPP processes have to also cope with the following two points:

- The accuracy of the real-time generated orbit and clock products is slightly worse than that of the post-processed products
- The extra difficulty associated to the communications channels functioning

This reinforces the message: the attainable absolute positioning accuracy of a real time PPP process fed with real-time generated products is in the range of a few centimetres.

FOUR EXAMPLE TEST CASES

This section shows the behaviour of the introduced KIPL algorithm in three different test scenarios: static PPP, PPP during convergence period and kinematic PPP (two different kinematic cases are shown). In each one of the considered cases, the percentage of integrity failures for different confidence levels is provided, together with integrity versus accuracy plots, showing the PPP horizontal/vertical errors and the associated KIPL protection levels for certain confidence levels.

These examples are aimed at illustrating the huge potential of the KIPL bounding algorithm in different environmental circumstances. Note that in all the considered cases, the KIPL configuration is the same, and that it is the algorithm itself that is capable of fitting all the considered circumstances: static, kinematic, convergence, multi-constellation, GPS-only and Glonass-only. Further extensive experimentation will be carried out supported by the promising initial results presented next:

Test Case 1: Static

The test is based on five days of data from the GAP1 station located in the GMV premises (see Figure 10, Figure 11). The configuration of the PPP process is the same as in the kinematic scenarios, the receiver not being assumed to be at rest. Table 1 contains the experimental rate of integrity failures for three confidence levels, for horizontal and vertical errors, which is below the target in all cases. Figure 12 and Figure 13 show the evolution of errors and PLs during the estimation arc for a confidence level of 99.9%. The typical value of the bound is of 10cm for horizontal errors and 20cm in the vertical case.

Finally, the last two figures show that even for a high level of confidence of 99.99999 the Protection Levels obtained are typically below half a meter in the horizontal direction and below 1m in vertical.

Figure 10: GAP1 Station

Figure 11: GAP1 Station Location

Table 1: Integrity failures in static scenario for different confidence levels

CL	95	99	99.9
H	1.79%	0.28%	0.0%
V	0.11%	0.01%	0.0%

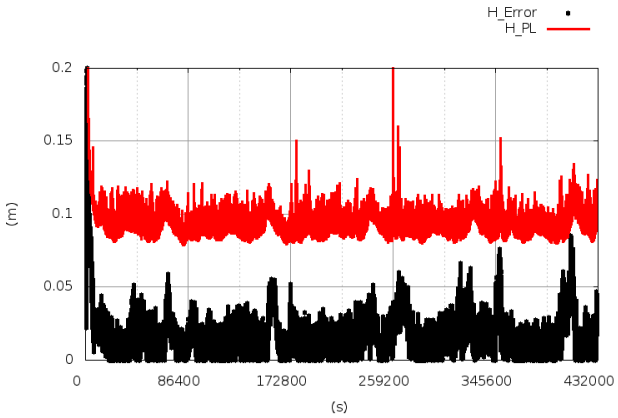

Figure 12: Horizontal performances, 99.9 confidence level, iono-free

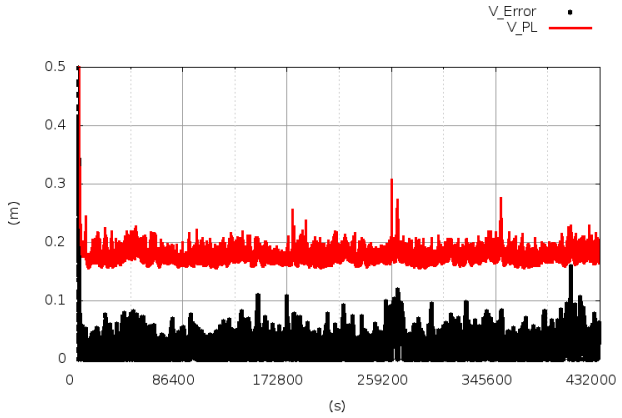

Figure 13: Vertical performances, 99.9 confidence level, iono-free

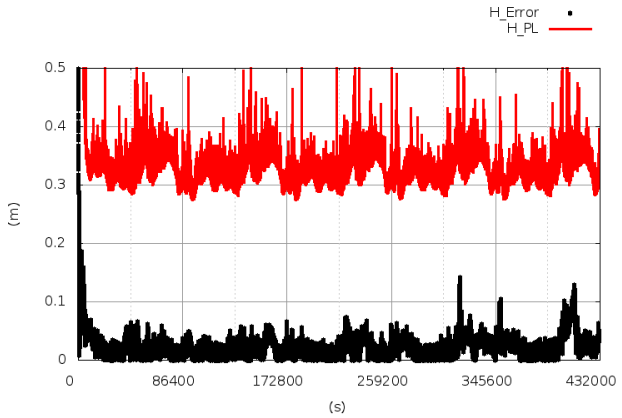

Figure 14: Horizontal performances, 99.99999 confidence level, iono-free

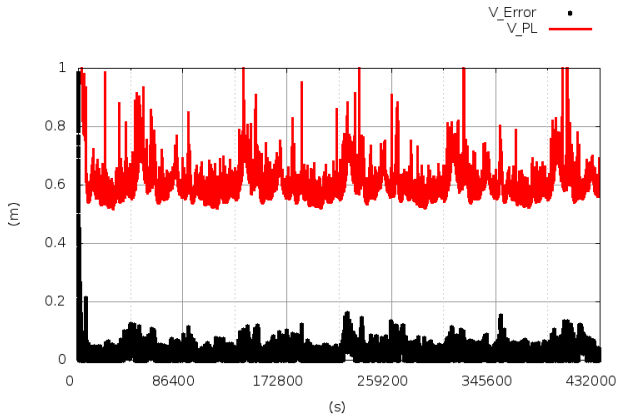

Figure 15: Vertical performances, 99.99999 confidence level, iono-free

Test Case 2: Convergence

An important feature of PPP navigation solutions is that the nominal accuracy is only reached after a period of time (‘convergence time’) that can range from a few minutes to more than half an hour, depending on the characteristics of the scenario. The integrity bounds should evolve accordingly, decreasing at a similar rate as the solution error. The results of current section show how

the integrity algorithm presented here also fulfils this requirement.

In order to analyse the behaviour of the Protection Levels during the period of convergence, the filter has been restarted every 2 hours. The results are fully satisfactory.

Table 2: Integrity failures in convergence scenario, GPS+GLONASS, for different confidence levels

CL	95	99	99.9
H	3.58%	0%	0%
V	1.43%	0.02%	0%

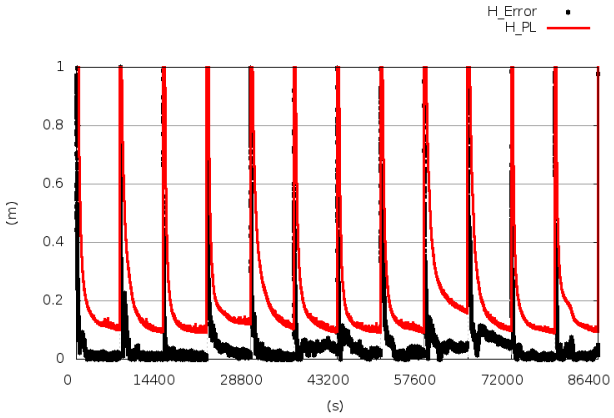

Figure 16: Horizontal performances, 99.9 confidence level, GPS+GLONASS

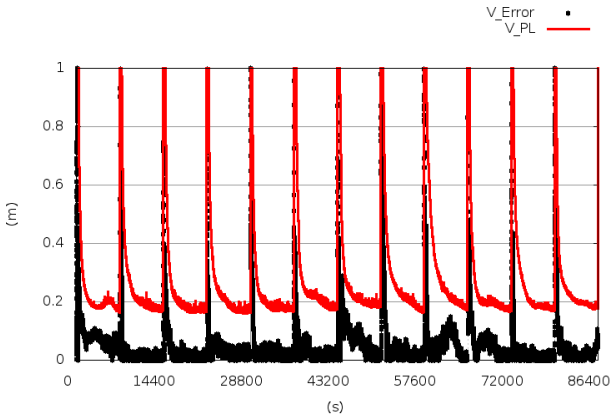

Figure 17: Vertical performances, 99.9 confidence level, GPS+GLONASS

In order to check the algorithm in different circumstances, the test has been repeated configuring either GPS or GLONASS satellites only. As the convergence may be slower, in the first case the filter has been reset every 4 hours, in the second every 8 hours. The results below show that the integrity bounds behave as expected.

Table 3: Integrity failures in convergence scenario, GPS-only, for different confidence levels

CL	95	99	99.9
H	1.38%	0%	0%
V	1.66%	0.05%	0%

Table 4: Integrity failures in convergence scenario, GLONASS-only, for different confidence levels

CL	95	99	99.9
H	3.86%	0.07%	0%
V	0.15%	0.01%	0%

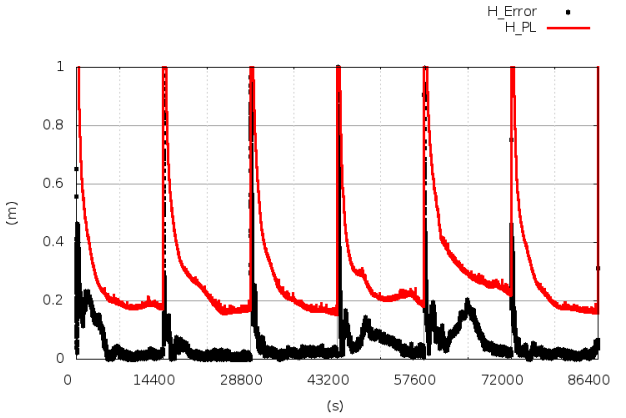

Figure 18: Horizontal performances, 99.9 confidence level, GPS-only

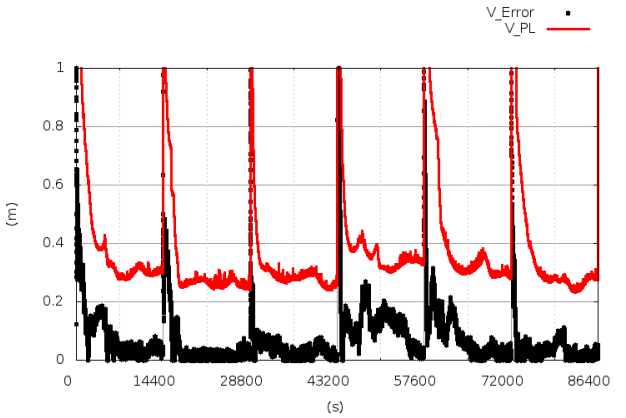

Figure 19: Vertical performances, 99.9 confidence level, GPS-only

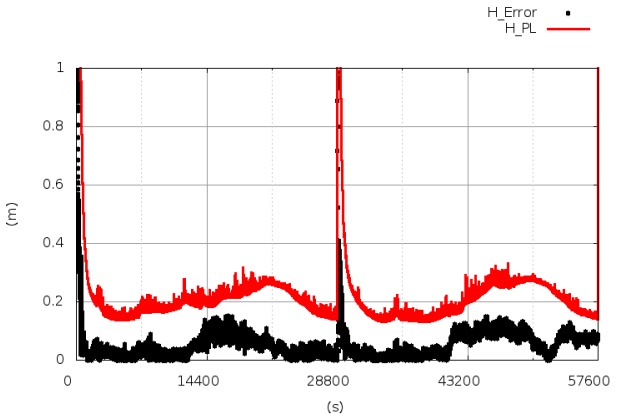

Figure 20: Horizontal performances, 99.9 confidence level, GLONASS-only

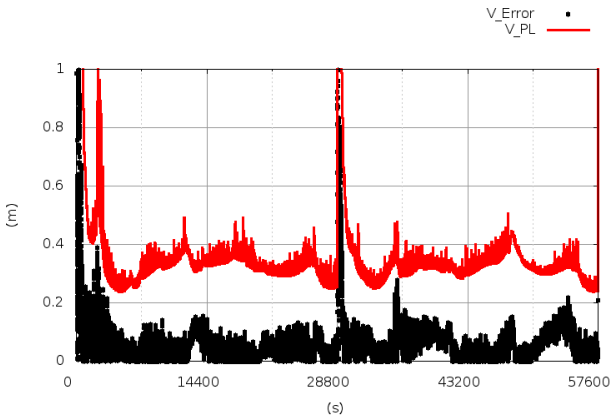

Figure 21: Vertical performances, 99.9 confidence level, GLONASS-only

Test Case 3: Kinematic_1

The second test case corresponds to a kinematic urban trajectory through Tres Cantos, the town were the GMV premises are located. It is about 20 km north from Madrid, the capital city of Spain, and it has an approximate population of about 42,000 inhabitants. The most common types of buildings are the blocks of apartments, and there are trees in the streets and avenues. Figure 22 below illustrates the urban characteristics of Tres Cantos.

Figure 22: Encuartes Avenue in Tres Cantos

The total scenario covers a whole period of about 2 hours. The pure kinematic part is a little bit more than 1 hour, whereas the first 50 minutes were reserved for ensuring convergence. The timeline of the test can be summarised as follows:

- Test starts: 03/09/2014 13:39:30 UTC
- Receiver is kept still for ensuring convergence
- Kinematic trajectory begins: 14:29:10 UTC
- Test ends: 15:35:00 UTC.

The followed trajectory is depicted below:

Figure 23: Kinematic Trajectory through Tres Cantos

As in the previously presented test case, the PPP process has been run in two different modes: iono-free combination, separate processing of double-frequency (DF) with gap-bridging mode activated. For each PPP process, in each one of the considered modes, the integrity/reliability algorithm has been run configured for three different confidence levels: 95, 99 and 99.9. Red colour has been used for depicting the obtained protection levels in some plots below illustrating the obtained results.

In parallel, an RTK process has been run with the aim of using it as reference for the associated accuracy and accuracy/integrity analyses. GAP1 has been used as base station. Its location is displayed in Figure 23 above, marked as "Reference Position" (south of Tres Cantos). The RTK solution is not continuous, since ambiguities have not been able to be solved for all the epochs in the considered time period. For this reason, there are some gaps in depicting the errors of the PPP processes when compared with respect to the RTK solution.

The obtained results have been summarised below. As in the previously presented test case, one table is provided for each one of the considered PPP processing modes. They show the percentage of integrity failures, for each one of the considered confidence levels (95, 99 and 99.9), in the horizontal and vertical directions. The percentages of integrity failures are displayed in red colour when the integrity/reliability threshold is exceeded and in black colour when it is not (5% for 95 confidence level, 1% for 99 and 0.1% for 99.9).

Table 5: Iono-free

CL	95	99	99.9
H	4.45%	0.16%	0.02%
V	0.38%	0.02%	0.02%

Table 6: separate DF with gap-bridging

CL	95	99	99.9
H	1.92%	0.05%	0.02%
V	0.20%	0.07%	0.02%

The following figures show the obtained results in terms of accuracy and integrity/reliability. Note that not all the plots have been included, for obvious space reasons, but a representative sampling is included next, showing the obtained results in the three processing modes, for the 99 confidence level, in the horizontal component:

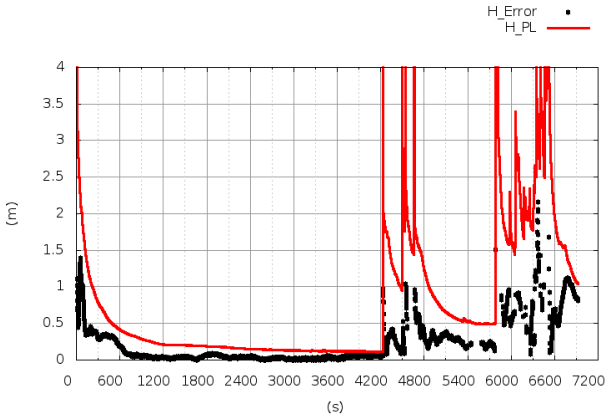

Figure 24: Horizontal performances, 99 confidence level, iono-free

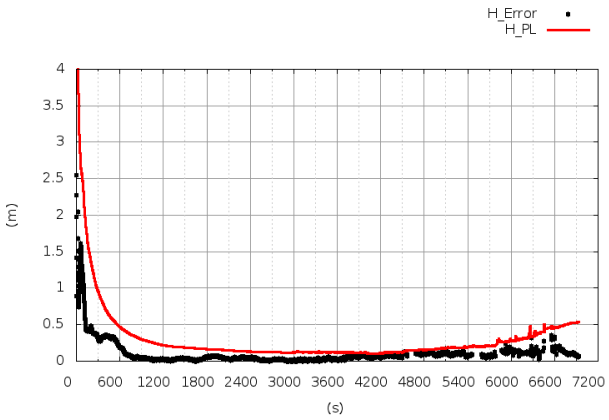

Figure 25: Horizontal performances, 99 confidence level, separate DF with gap-bridging

It is especially interesting to pay attention on the magnitude of the obtained protection levels, which soon decrease below 1 metre while converging and stay below 0.5 m in good observability conditions. When the observability conditions start getting complicated, differences can be appreciated in the two PPP processing modes. The performances are much better in the second case, when the gap-bridging mode is activated.

A zoom of Figure 25 is also included, limiting the y-axis to 1 m, for a more detailed perspective:

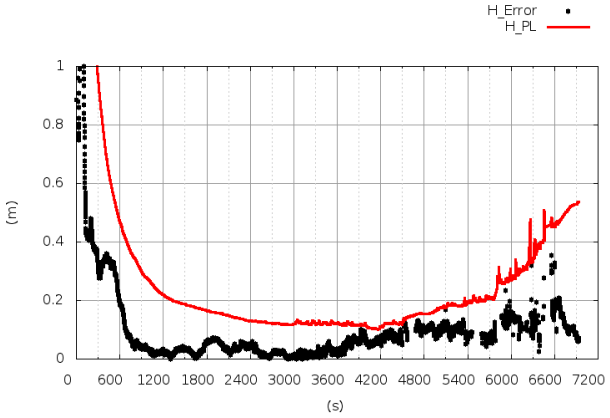

Figure 26: Zoom of Figure 25, limiting y-axis to 1 m

Test Case 4: Kinematic 2

The third test case corresponds to a new kinematic trajectory, starting in Tres Cantos and finishing in Colmenar Viejo, a nearby town less than 10 km away, passing several times below a rail bridge, before leaving Tres Cantos, and passing below two more bridges, one of them in the first kilometres of the road connecting the two towns, and the other one when arriving to Colmenar Viejo. The followed trajectory is depicted below:

Figure 27: Kinematic Trajectory Tres Cantos - Colmenar Viejo

The rail bridge which has been used as location for this test case is shown in Figure 28 below:

Figure 28: Rail bridge

The total scenario covers a whole period of about 2 hours. The pure kinematic part is about 1 hour and 15 minutes, whereas the first 45 minutes were reserved for ensuring convergence. The timeline of the test can be summarized as follows:

- Test starts: 19/05/2015 09:45:30 UTC.
- From 10:34:56 to 11:23:28 UTC the vehicle passes 10 times below the rail bridge shown in Figure 28 above. The bridge is located between two roundabouts, and the vehicle goes from one to the other five times, passing have the times below the bridge in in one direction, and half the times in the other one. The vehicle remains stopped for about 4-5 minutes before and after driving below the bridge in one of the directions, in order to space the passes. The passes take place at the following times:
    - 10:34:56-10:34:59 UTC (going).
    - 10:41:39-10:41:41 UTC (coming).
    - 10:49:59-10:50:01 UTC (going).
    - 10:56:42-10:56:45 UTC (coming).
    - 11:04:17-11:04:19 UTC (going).
    - 11:09:20-11:09:22 UTC (coming).
    - 11:14:00-11:14:05 UTC (going).
    - 11:18:40-11:18:43 UTC (coming).
    - 11:22:38-11:22:43 UTC (going).
    - 11:23:25-11:23:29 UTC (coming).
- Then the vehicle drives through Tres Cantos on its way out to the road to Colmenar.
- The vehicle passes below a road bridge (11:28:24-11:28:27 UTC) which is not yet in the Google maps, since it has been recently built.
- The vehicle passes below a road bridge again, at 11:33:19 UTC, just before arriving to Colmenar Viejo.
- Colmenar Viejo is reached at about 11:35:25 UTC.
- The vehicle stops at 11:42:46 UTC and it remains stopped until the end of the test.
- Test finishes at 11:44:11 UTC.

As in the previously presented test cases, the PPP process has been run in three different modes: iono-free combination, separate processing of double-frequency (DF) with iono estimation and separate processing of double-frequency (DF) with iono estimation plus gap-bridging mode activated. Again RTK has been used for generating a reference trajectory, again discontinuous because not all ambiguities have been able to be correctly fixed, and the same colour code as in the previous test cases has been used for plotting the results.

The obtained results in terms of integrity failures, as the previous test case, are summarized in the tables below:

Table 7: Iono-free

CL	95	99	99.9
H	3.02%	0.02%	0.02%
V	4.22%	0.02%	0.02%

Table 8: separate DF with gap-bridging

CL	95	99	99.9
H	0.04%	0.04%	0.02%
V	3.23%	0.13%	0.02%

Again some figures are presented illustrating some of the obtained results. The plots show the obtained results in the three processing modes, for the 99.9 confidence level, in the vertical component:

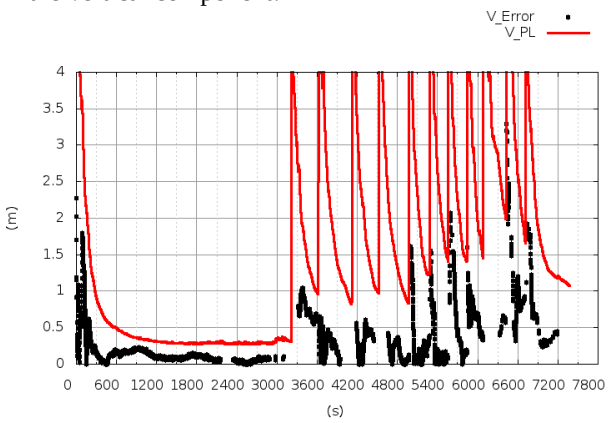

Figure 29: Vertical performances, 99.9 confidence level, iono-free

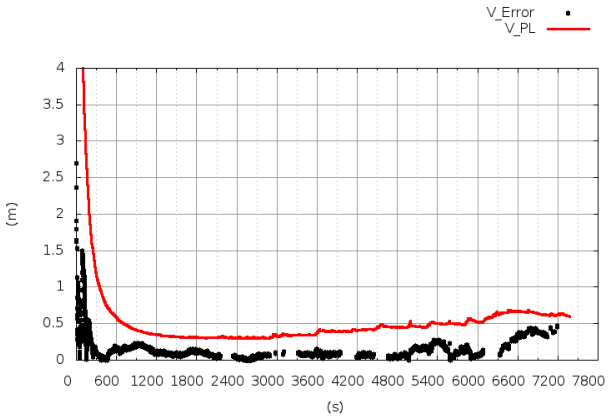

Figure 30: Vertical performances, 99.9 confidence level, separate DF with gap-bridging

A zoom of Figure 30 is also included, limiting the y-axis to 1 m, for a more detailed perspective:

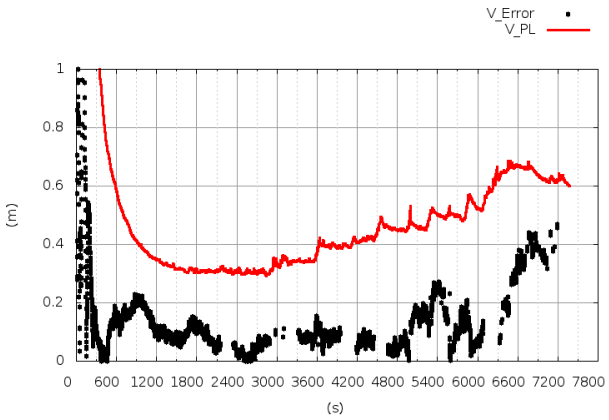

Figure 31: Zoom of Figure 30, limiting y-axis to 1 m

The obtained results are completely coherent with the ones obtained in the previous test case. Again it is observed that relatively small (submetric) protection levels are being provided by the PPP integrity/reliability algorithm. Better results are obtained when the two frequencies are processed separately, and the iono is estimated instead of performing the iono-free combination, and PLs decrease much faster when the gap-bridging mode is activated.

FURTHER WORK

Now that he have obtained a rigorous formulation for PPP integrity/reliability, and once that we have successfully tested it in some preliminary real scenarios, both open-sky, as well as in more demanding kinematic urban and road trajectories, it is the time to carry out an extensive experimentation, which will include:

- Extensive analysis in static scenario, compiling a large data set (several months) and allowing different integrity/reliability analyses such as Stanford diagrams, and safety index vs number of integrity failures charts.
- Extensive analyses in kinematic scenarios, including:
  - Galileo satellites in the process. The Galileo signal E5 is robust in circumstances where the GPS L2 signal can be lost, see [Ref. 8.].
  - More challenging road and urban environments.
- Further research for higher confidence levels

If the promising results of the newly introduced PPP bounding computation get to be further consolidated, the PPP integrity/reliability algorithm will be able to be considered an excellent balanced candidate half way between the system and the user integrity solutions, enriching the current offer of integrity for navigation solutions.

In parallel to the mentioned extensive experimentation activities, and enriched with the generated feedback, continuous improvement of all the PPP related functionalities will be carried out, including:

- OD&TS process improvement, in order to ensure excellent orbit and clock products performances
- PPP process improvement, in order to enhance the robustness and accuracy of the provided solutions, both for double and single frequency applications
- PPP integrity/reliability algorithm refinement, for being able to cope with the widest range of difficulties in all kind of environments

CONCLUSIONS

- PPP is consolidated as an alternative/complement to RTK high positioning technique.
- PPP is able to work in static and kinematic scenarios, both in real-time and in post-processing modes, for many different highly demanding applications.
- PPP positioning performances are better than 10 cm (horizontal) and better than 15 cm (vertical), 95%, after 20 minutes convergence period.
- The high accuracy of the PPP solutions and the robustness for the PPP processes has allowed the definition of a rigorously formulated reliability bound computation algorithm.
- The obtained reliability bounds are in the range of a few decimeters, providing integrity failures percentages in the required intervals for different confidence levels in the analysed scenarios.
- Further experimentation will be carried out, motivated by the excellent preliminary test results presented in this paper.
- The results of the mentioned further extensive experimentation will result in valuable feedback for improving all the PPP related functionalities: OD&TS, PPP processing and PPP bound computation.
- If the promising results of the newly introduced PPP bounding computation get to be further consolidated, the PPP integrity/reliability algorithm will be able to be considered an excellent balanced candidate half way between the system and the user integrity solutions, enriching the current offer of integrity for navigation solutions.

REFERENCES

[Ref. 1.] “Method for Autonomous Determination of Protection Levels for GNSS Positioning Based on Navigation Residuals and an Isotropic Confidence Ratio” Patent: Europe: EP2113786 (B1), USA: US8203482 (B2).

[Ref. 2.] “Method for computing an error bound of a Kalman filter based GNSS position solution” Pending Patent: Europe EP14189240.6.

[Ref. 3.] Píriz, R., Mozo, A., Navarro, P., Rodríguez, D., "magicGNSS: Precise GNSS Products Out of the Box," *Proceedings of the 21st International Technical Meeting of the Satellite Division of The Institute of Navigation (ION GNSS 2008)*, Savannah, GA, September 2008, pp. 1242-1251.

[Ref. 4.] Tobías, Guillermo, Calle, J. David, Navarro, Pedro, Rodríguez, Irma, Rodríguez, Daniel, "magicGNSS' Real-Time POD and PPP Multi-GNSS Service," *Proceedings of the 27th International Technical Meeting of The Satellite Division of the Institute of Navigation (ION GNSS+ 2014), Tampa, Florida, September 2014*, pp. 1046-1055.

[Ref. 5.] Píriz, R., Calle, D., Mozo, A., Navarro, P., Rodríguez, D., Tobías, G., "Orbits and Clocks for GLONASS Precise-Point-Positioning, *"Proceedings of the 22nd International Technical Meeting of The Satellite Division of the Institute of Navigation (ION GNSS 2009)*, Savannah, GA, September 2009, pp. 2415-2424.

[Ref. 6.] Tobias, Guillermo, Garcia, Cristina, Mozo, Alvaro, Navarro, Pedro, Piriz, Ricardo, Rodriguez, Irma, Rodriguez, Daniel, *"Filling in the gaps of RTK with Regional PPP," Proceedings of the 24th International Technical Meeting of The Satellite Division of the Institute of Navigation (ION GNSS 2011)*, Portland, OR, September 2011, pp. 2193-2201.

[Ref. 7.] Mozo, Álvaro, Calle, J. David, Navarro, Pedro, Píriz, Ricardo, Rodríguez, Daniel, Tobías, Guillermo, "Demonstrating In-The-Field Real-Time Precise Positioning," *Proceedings of the 25th International Technical Meeting of The Satellite Division of the Institute of Navigation (ION GNSS 2012)*, Nashville, TN, September 2012, pp. 3066-3076.

[Ref. 8.] Tobías, Guillermo, Calle, J. David, Navarro, Pedro, Rodríguez, Irma, Rodríguez, Daniel, "Real-Time PPP with Galileo, Paving the Way to European High Accuracy Positioning," *Proceedings of the 27th International Technical Meeting of The Satellite Division of the Institute of Navigation (ION GNSS+ 2014)*, Tampa, Florida, September 2014, pp. 2354-2362.

[Ref. 9.] Merino, Miguel M. Romay, Lainez, Maria D., "Integrity for Advanced Precise Positioning Applications," *Proceedings of the 25th International Technical Meeting of The Satellite Division of the Institute of Navigation (ION GNSS 2012)*, Nashville, TN, September 2012, pp. 2742-2758.

[Ref. 10.] Samper, M. D. Laínez, Romay Merino, M. M., "In-The-Field Trials for Real-Time Precise Positioning and Integrity in Advanced Applications, *"Proceedings of the ION 2013 Pacific PNT Meeting"*, Honolulu, Hawaii, April 2013, pp. 146-167.

[Ref. 11.] Laínez Samper, María D., Romay Merino, Miguel M., Tobías González, Guillermo, Barba Martí, David, "PPP for Advanced Precise Positioning Applications, Including Reliability Bound," *Proceedings of the 27th International Technical Meeting of The Satellite Division of the Institute of Navigation (ION GNSS+ 2014)*, Tampa, Florida, September 2014, pp. 2478-2493.

[Ref. 12.] Cosmen-Schortmann, J.; Azaola-Saenz, M.; Martinez-Olague, M.A.; Toledo-Lopez, M.; , "Integrity in urban and road environments and its use in liability critical applications," Position, Location and Navigation Symposium, 2008 IEEE/ION , vol., no., pp.972-983, 5-8 May 2008, DOI: 10.1109/PLANS.2008.4570071

[Ref. 13.] Isotropy-Based Protection Levels: a Novel Method for Autonomous Protection Level Computation with Minimum Assumptions, Azaola Sáenz, M.; Cosmen Schortmann, J.; Martínez Olagüe, M.A.; Toledo López, M., GMV Aerospace and Defence S.A. (Spain), NAVITEC 2008, Noordwijk (The Netherlands), Dec 2008.

[Ref. 14.] Azaola Sáenz, M., Cosmen Schortmann, J. "Autonomous Integrity, An Error Isotropy-Based Approach for Multiple Fault Conditions, Inside GNSS, http://www.insidegnss.com/auto/janfeb09-azaoli.pdf January/February 2009, pp.28-36.

[Ref. 15.] Azaola, M., Calle, D., Mozo, A., Piriz, R., "Autonomous Isotropy-Based Integrity Using GPS and GLONASS, *"Proceedings of the 23rd International Technical Meeting of The Satellite Division of the Institute of Navigation (ION GNSS 2010)*, Portland, OR, September 2010, pp. 2135-2147.

[Ref. 16.] .Navarro, P., Azaola, M., Moriana, C., Cosmen, J., "Computing Meaningful Integrity Bounds of a Low-cost Kalman-filtered Navigation Solution in Urban Environments", pending on final acceptance under peer review process for *ION GNSS+ 2015 Proceedings*.

[Ref. 17.] ESA Navipedia, European Space Agency. navipedia.net

[Ref. 18.] http://www.gmv.com/en/space/Satellite_navigation_systems/GNSS_tools_development.html

[Ref. 19.] RTKLib by Tomoji Takasu (*gpspp.sakura.ne.jp/rtklib/rtklib.htm).*

[Ref. 20.] IERS Earth Orientation Data http://www.iers.org/IERS/EN/DataProducts/EarthOrientationData/eop.html

[Ref. 21.] IERS Conventions 2010, http://www.iers.org/IERS/EN/Publications/TechnicalNotes/tn36.html